Journal of Geography and Geology; Vol. 7, No. 1; 2015
ISSN 1916-9779 E-ISSN 1916-9787
Published by Canadian Center of Science and Education

Potential for Estimating the Thickness of Freshwater Lake Ice by GPS Interferometric Reflectometry

Mark D. Jacobson[1]

[1] Department of Mathematics, Montana State University Billings, Billings, MT, USA

Correspondence: Mark D. Jacobson, Department of Mathematics, Montana State University Billings, Billings, MT, 59101, USA. Tel: 1-406-657-2203. E-mail: mjacobson@msubillings.edu

Received: September 13, 2014 Accepted: September 30, 2014 Online Published: January 25, 2015
doi:10.5539/jgg.v7n1p10 URL: http://dx.doi.org/10.5539/jgg.v7n1p10

Abstract

The potential for inferring the thickness of freshwater lake ice by the global positioning system (GPS) is explored. Specifically, lake ice thickness is inferred by using measured GPS signals and calculated results from an interferometric reflectometry (IR) model. The difference of these two quantities is minimized with a nonlinear least squares fitting algorithm. Only low elevation angles (≤ 25°) of received GPS signals are used in this study. The possibility of estimating lake ice thickness by using the received GPS signals from satellite PRN 10 and the GPS-IR model is demonstrated from a 1-day experiment. For this satellite, the average inferred ice thickness (38.0 cm) slightly underestimated the *in situ* measurements (39.4 cm ± 1.3 cm). GPS satellites PRN 2 and PRN 24 are also used in this study. However, signals from these satellites significantly underestimated the *in situ* measurements.

Keywords: global positioning system, freshwater lake ice thickness, specular reflection

1. Introduction

Freshwater lake ice information is important in the northern hemisphere. For example, the meteorogical conditions in the northern latitudes may be related to the ice thickness in lakes and rivers (Palecki & Barry, 1986; Hall, Fagre, Klasner, & Liston, 1994). In the United States, the National Oceanic and Atmospheric Administration's (NOAA) Great Lakes Environmental Research Laboratory (GLERL) of the Department of Commerce (DOC) has operated and managed the synoptic ice chart observations for the Great Lakes of North America for approximately 50 years (Assel, 2005). This critical lake ice information is important because of the ice cover's extent and duration has a major impact on the economy of this region. In particular, lake ice cover can impede commercial navigation; interfere with hydropower production and cooling water intakes; and damage shore structures. In addition, ice cover impacts the water balance of the lakes. This occurs because ice cover affects mass and energy transfers to the lakes and from the lakes (Assel, 2004). In short, better lake ice measurements will improve the understanding of ice cover climatology and forecasts of winter lake ecosystems.

The measurement of freshwater lake ice thickness is also important for ice roads in the northern latitudes (Finlay, Parry, Proskin, & Mickle, 2008; Mala, 2007). The communities in these regions depend upon the ice roads in the winter season for various supplies. Specicially, these regions require food, medical equipment, housing items, fuel, tools, and machinery to primarily support the extraction and exploration of gas, oil, and diamonds. Although manual drilling can used to measure the thickness of lake ice, ground penetrating radars (GPR) requires much less manual labor, is cheaper and provides better spatial data. It is interesting that the Mala's (2007) GPR frequency (1.6 GHz) is similar to the GPS L1 frequency (1.57542 GHz).

Conventional remote sensing techniques using radars and radiometers are typically used to infer the thickness of ice on frozen lakes and rivers (Arcone, Yankielun, & Chacho, 1997; Hall, Fagre, Klasner, & Liston, 1994; Arcone, 1991; Riek, Crane, & O'Neill, 1990; Hall, Foster, Chang, & Rango, 1981; Swift, Jones, Harrington, Fedors, & Couch, 1980; Apinis & Peake, 1976; Cooper, Mueller, & Schertler, 1976). Recently, the reflected signals of the global navigation satellite systems (GNSS-R) are being used to sense the Earth's cryosphere (Jin, Feng, & Gleason, 2011; Cardellach et al., 2011; Jin & Komjathy, 2010; Gleason & Gebre-Egziabher, 2009; Gleason, Lowe, & Zavorotny, 2009). For example, estimating snow depth by using the reflected GPS signals is showing great promise (McCreight, Small, & Larson, 2014; Nievinski & Larson, 2014a; Nievinski & Larson, 2014b; Larson & Nievinski, 2012; Rodriguez-Alvarez et al., 2012; Gutmann, Larson, Williams, Nievinski, &

Zavorotny, 2011; Fabra et al., 2011; Larson et al., 2009; and Jacobson, 2008). These reflected GPS signals may also provide useful information about freshwater lake ice thickness (Jacobson, 2010). This would increase the temporal and spatial coverage of remotely sensing frozen lake thickness compared to the current techniques. In this paper, a GPS interferometric reflectometry (GPS-IR) technique is used to attempt inferring freshwater lake ice thickness (Gutmann, Larson, Williams, Nievinski, & Zavorotny, 2011). This technique produces an interference pattern by receiving both reflected and direct GPS signals simultaneously. Information about the subsurface, such as lake ice thickness, can be obtained by analyzing this interference signal. In particular, Jacobson (2010) states "For example, inferring ice thickness might be possible by using the first deep fade's elevation angle value and a least squares fit between theory and measurement over a specified elevation angle range." This statement is explored in the following sections.

2. Theory

Estimating freshwater lake ice thickness is explored by using the model given by Jacobson (2010). The total right-hand circularly polarized (RHCP) field at the vertically mounted GPS receiving antenna is the sum of the direct and specularly reflected signals (see Figure 1). The reflected signal amplitude is a function of the elevation angle θ and the combination of the snow layer, the ice layer and the water. The reflected power calculation does not include rough surface scattering or incoherence; i.e., only smooth, flat horizontal surfaces are used (Ulaby, Moore, & Fung, 1986). Therefore, with these simplifications, only the specular point within the first Fresnel zone is considered in this model. In contrast, the received GPS power measurements do include rough surface scattering and incoherence.

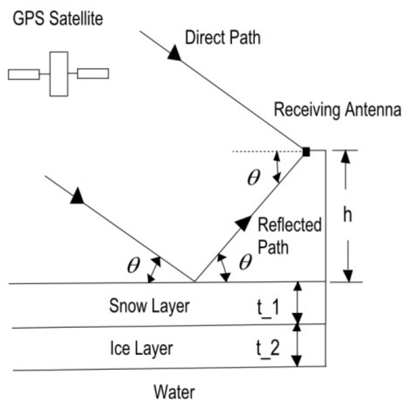

Figure 1. Geometry of the GPS-IR technique

The relative power (normalized to the maximum signal level) at the RHCP receiving antenna is (Jacobson, 2010; Stutzman, 1993) is

$$P = \left|1 + \frac{(r_{\mathrm{h}} - r_{\mathrm{v}})}{2} \exp\,(i\phi)\right|^2 \tag{1}$$

where 1 is the relative RHCP field component from the direct path; r_{h} is the reflected horizontally polarized field component; r_{v} is the reflected vertically polarized field component; $\phi = \frac{4\pi h sin\theta}{\lambda_0}$ is the phase shift difference between the direct and reflected paths (Beckmann & Spizzichino, 1987); $i = \sqrt{-1}$ by definition; h is the antenna height above the air-snow interface (m); θ is the elevation angle (degrees); $c = 2.997925 \times 10^8$m/s is the speed of light in a vacuum; $f = 1.57542$GHz is the GPS L1 frequency; and $\lambda_0 = c/f = 0.1902937$ m is the GPS L1 wavelength.

The input variables contained in (1) are the dry snow's relative complex permittivity (ε_{s}) with a temperature of -2.2°C and a relative snow density of 0.24 g cm^{-3}, the freshwater lake ice's relative complex permittivity ($\varepsilon_{\mathrm{ice}}$) with a temperature of -2.2°C, the liquid water's relative complex permittivity (ε_{w}) with a temperature of 0°C , the snow layer thickness (t_1 in m), and the ice layer thickness (t_2 in m). The dry snow and liquid water parameters are given in Jacobson (2010). The relative complex permittivity value of freshwater ice used in this study is (Matzler & Wegmuller, 1987)

$$\varepsilon_{\text{ice}} = \varepsilon'_{\text{ice}} - i\varepsilon''_{\text{ice}} \tag{2}$$

where

$$\varepsilon'_{\text{ice}} = 3.17 \tag{3}$$

$$\varepsilon''_{\text{ice}} = \frac{A}{f} + Bf^{c} \tag{4}$$

where f is the frequency in GHz; A = 0.0026, B = 0.00023, and C = 0.87 for temperatures of -5°C. The fixed input parameters from Jacobson (2010) and (2) are given in Table 1.

Table 1. Fixed parameters in model

ε_s	ε_{ice}	ε_w	t_1 (cm)	h (cm)
$1.48 - i2.71\times10^{-4}$	$3.17 - i1.99\times10^{-3}$	$85.57 - i14.12$	0.3	50.5

3. Inferring Freshwater Lake Ice Thickness

A Trimble Lassen LP receiver was used in this study. The GPS antenna specifications are given in Jacobson (2014). The GPS receiver output power levels in decibels (dB) every 0.5 s to a computer. A photograph of the frozen lake with a thin snow layer at Cooney Reservoir and the vertically-mounted receiving antenna is shown in Figure 2. The vertically-mounted antenna provides equal gain for the direct and speculary reflected signals. This reservoir is approximately 80 km southwest of Billings, MT, USA. On the day of the measurements (February 13, 2009), the interfaces between the air, snow and ice were visually smooth compared to 19 cm (the GPS L1 wavelength). In addition, the ice-water interface is also assumed to be smooth (Cooper, Mueller, & Schertler, 1976). The azimuthal bore-sight angle of the receiving antenna was 100°. The antenna was mounted vertically on a tripod at the height given in Table 1. With this antenna height at GPS elevation angle of 5° (lowest elevation angle used in this study), the first Fresnel zone has a major axis length of about 35 m and a minor axis length of about 3 m. The Fresnel zone ellipse becomes smaller and closer to the antenna with larger elevation angles.

Figure 2. Photograph of Cooney Reservoir during the measurements

Since the reservoir's shore is greater than 200 m from the antenna, the first Fresnel zone lies entirely on the frozen lake. Terrain blockage and shadowing were negligible at this site for the GPS elevation angles of interest. The received power is normalized to the calculated power to facilite estimating lake ice thickness. As described in Jacobson (2010), the measured ice thickness was approximately 39.4 cm $\pm$ 1.3 cm.

The sky plot of satellites PRNs 2, 10 and 24 is shown in Figure 3, where the elevation (EL) and azimuth (AZ) angles are from each satellite and the radial distance (RD) is from the receiving antenna. Sky plots show the specular reflection points on the frozen lake as referenced from the receiving antenna (Larson & Nievinski, 2012). The three GPS satellites have azimuth angle tracks close to the azimuthal bore-sight angle of the receiving antenna of 100°. Table 2 shows the angular ranges of the satellites for the ~1 h measurements. The measurements were collected with partly cloudy skies.

Table 2. Angular ranges of GPS satellites during measurements

PRN	Time (GPS)		AZ (Degrees)		EL (Degrees)	
	Start	End	Start	End	Start	End
2	17:40	18:36	74	88	25	5
10	19:15	20:08	53	59	25	5
24	21:01	21:56	115	128	25	5

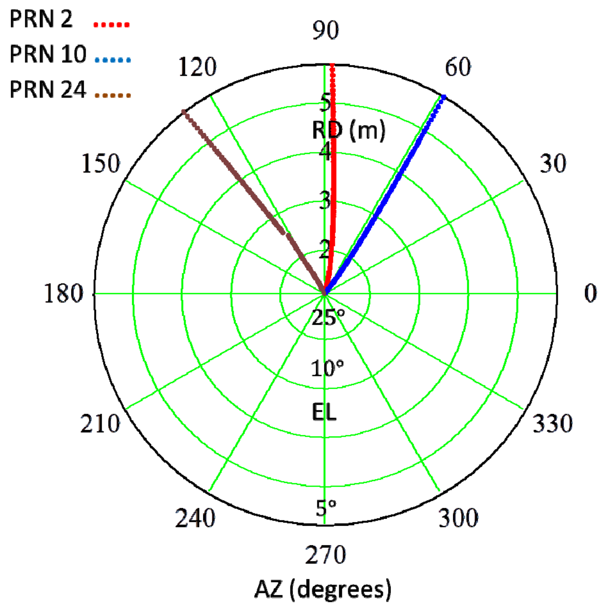

Figure 3. Sky plot of the three GPS satellites; in situ measurements are located near the center of the plot (backside of the antenna) along the 0° azimuth

A quasi-Newton algorithm (QNA) (Herceg, Krejic, & Luzanin, 1996; Martinez, 1990) is used to compare the received power signals and the modelled power signals given in (1). The specular reflection effects from the ice layer were maximimzed by restricting the elevation angles to be between 5° and 25°. At these angles, the electrical path length of the signal is greater than those at larger elevation angles. This range of elevation angles has been used in several GNSS-R snow sensing experiments (Larson and Nievinski (2012); Gutmann, Larson, Williams, Nievinski, and Zavorotny (2011); and Larson et al., (2009)). For this experiment, the number of data points received from satellites PRNs 2, 10 and 24 were 3 369, 3 132, and 3 108, respectively.

The following equation is used in the QNA to infer lake ice thickness (Jacobson, 2014):

$$PdB = 10\log\left(P/Norm\right) \tag{5}$$

where P is given in (1), and $Norm$ is a constant between 2 and 4. For each ice layer thickness, the $Norm$ value minimizes the errors in the constraints (Martinez, 1990). The $Norm$ constant helps to minimize the error between measurement data and the theoretical calculations. Approximately 120 different ice thickness values, within the range 20 – 70 cm, are chosen for the inputs to a QNA. These ice layer thicknesses are similar to those of Cooper, Mueller, and Schertler (1976); and Hall, Foster, Chang, and Rango (1981). A QNA mimimizes the difference between measurement and theory by using a nonlinear least square fit. For each ice thickness value, the QNA outputs a standard error (SE) as follows (Jacobson, 2014):

$$\mathrm{SE}(Norm) = minimize\left\{\sqrt{\frac{1}{n-2}\sum_{i=1}^{i=n}[y(\theta_i) - PdB(\theta_i, Norm, t_1, t_2, \rho_\mathrm{d}, \varepsilon_\mathrm{ice}, \varepsilon_\mathrm{w}, T, f)]^2}\right\} \tag{6}$$

where y is the relative measured power value in dB; PdB is given in (5), in dB; θ_i is the elevation angle in degrees; $t_1, t_2, \rho_\mathrm{d}, \varepsilon_\mathrm{ice}, \varepsilon_\mathrm{w}, T, f$ are given in Section 2; n is the number of data points received from each satellite.

The smallest SE value from the 120 different ice thicknesses provides the best estimate of ice thickness. A graph of the SE values from these different ice thicknesses for PRN 10 is shown in Figure 4; on top of each ice layer is a 0.3 cm thick snow layer. Ice thickness values of 34.85 and 41.20 cm both produce a minimum SE of 0.63 dB. The arithmetical average value of these two values produces an ice thickness of 38.0 cm. This average inferred ice thickness is very close to the minimum value of the *in situ* measurements of 38.1 cm (39.4 cm $\pm$ 1.3 cm). It is interesting to note that the ice thickness difference between two consecutive minimum SE values is approximately $\lambda_0/3$, where $\lambda_0 \sim 19$ cm. Further investigation may determine is this a significant result. Figure 5 is a graph of the 8 minimum SE values (see Figure 4) versus ice thickness; these 8 SE values are connected using Microsoft Excel's smoothing function. The inferred ice thickness of 38.0 cm is located at the minimum SE value in Figure 5. This indicates that the simple layered model in Section 2 may be representative of the actual ice thickness profile for this GPS azimuth track (53° - 59°) (Cooper, Mueller, & Schertler, 1976; Bengtsson, 1986). The measurements and the theoretical results for ice thicknesses of 34.85 and 41.20 cm for PRN 10 are shown in Figure 6.

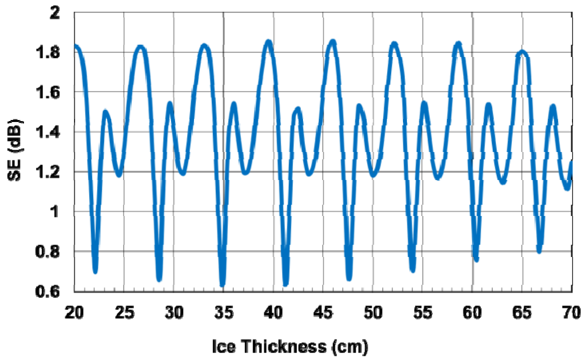

Figure 4. Plot of ice layer thickness versus SE

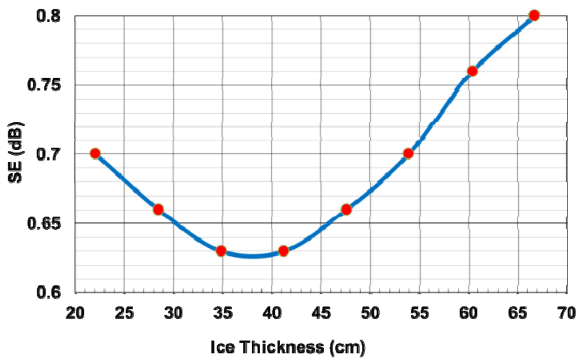

Figure 5. Plot of 8 minimum SE values (red circles) from Figure 4

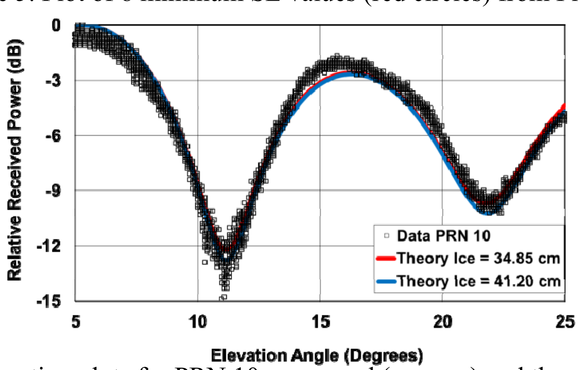

Figure 6. Elevation plots for PRN 10, measured (squares) and theoretical (lines)

A graph of the SE values from the 120 ice thicknesses for PRN 2 is shown in Figure 7; on top of each ice layer is a 0.3 cm thick snow layer. In this case, the inferred ice thickness is approximately 22.4 cm. This inferred ice thickness is clearly outside the measurement values (39.4 cm ± 1.3 cm). This is further emphasized in Figure 8 when the 8 minimum SE values (see Figure 7) are plotted as a function of ice thickness. Furthermore, Figure 8 shows that the inferred ice thickness values agree better for ice thickness values close to 20 cm and 70 cm. The incorrect ice thickness estimate of 22.4 cm may indicate that the lake ice thickness may be nonuniform for this GPS azimuth track (74° - 88°). Nonuniform lake ice thickness does occur. For example, Hall, Fagre, Klasner, and Liston (1994) reported that Lake McDonald in northern Montana, United States had thinner ice in the lake's southwestern region (~ 15 cm) than in the lake's northeastern region (~ 29 cm). This is an ice thickness variation of 14 cm. Furthermore, Bengtsson (1986) reported that an ice thickness range of 5 – 10 cm is common for a lake. Arcone, Yankielun, and Chacho (1997) also reported varied lake ice thicknesses for Lake 06 near Prudhoe Bay in northern Alaska, United States. These variable ice thickness ranges of 5 – 14 cm are on the order of the GPS L1 frequency of 19 cm. Therefore the simple layered model does not appear to be representative of the actual spatial variation of ice thickness for the PRN 2 azimuth track. In future experiments, more manually drilled ice holes need to done at various locations within the first Fresnel zone to verify the actual ice thickness. The measurements and the theoretical results for an ice thickness of 22.4 cm for PRN 2 are shown in Figure 9. Clearly, these results do not agree as well as those shown in Figure 6.

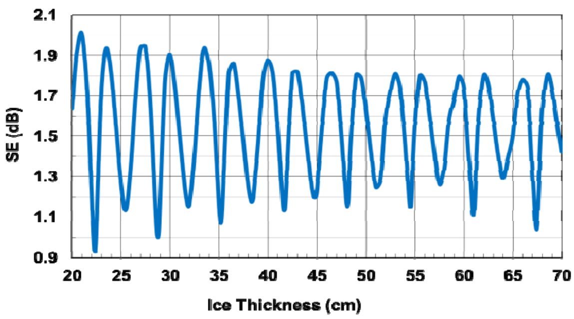

Figure 7. Plot of ice layer thickness versus SE

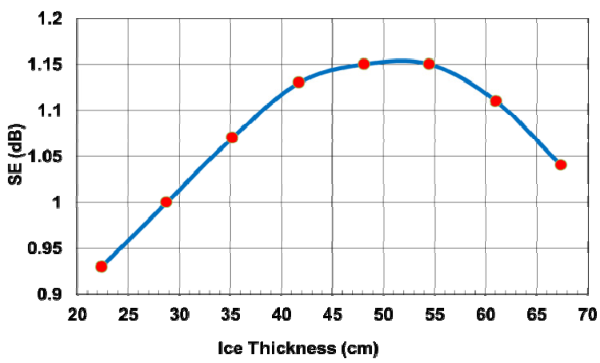

Figure 8. Plot of 8 minimum SE values (red circles) from Figure 7

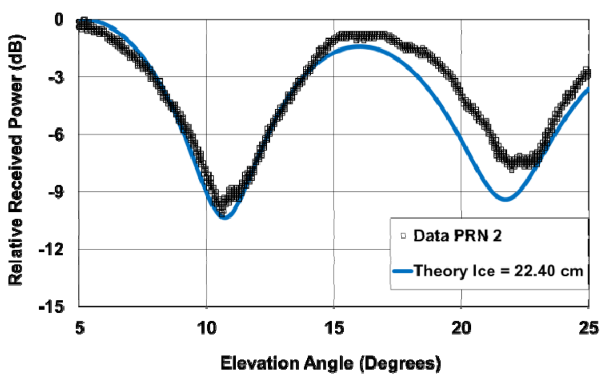

Figure 9. Elevation plots for PRN 2, measured (squares) and theoretical (line)

A graph of the SE values from the 120 ice thicknesses for PRN 2 is shown in Figure 10; on top of each ice layer is a 0.3 cm thick snow layer. In this case, the inferred ice thickness is approximately 25.3 cm. This inferred ice thickness is also outside the measurement values (39.4 cm $\pm$ 1.3 cm). This is further emphasized in Figure 11 when the 8 minimum SE values (see Figure 10) are plotted as a function of ice thickness. Furthermore, the inferred ice thickness values agree better for ice thickness values close to 20 cm and 70 cm. Similar to PRN 2's results, the incorrect inference of ice thickness of 25.3 cm may indicate that the lake ice thickness may be nonuniform for this GPS azimuth track (115° - 128°). Therefore, the simple layered model does not appear to be valid when attempting to estimate lake ice thickness for the PRN 24 azimuth track. The measurements and the theoretical results for an ice thickness of 25.3 cm for PRN 24 are shown in Figure 12. These results do not agree as well as those shown in Figure 6. Table 3 shows the inferred values of lake ice thickness and SE for the three GPS satellite tracks; the *in situ* measurements are also shown.

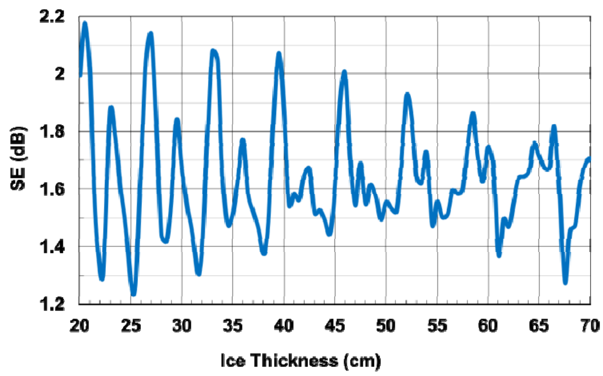

Figure 10. Plot of ice layer thickness versus SE

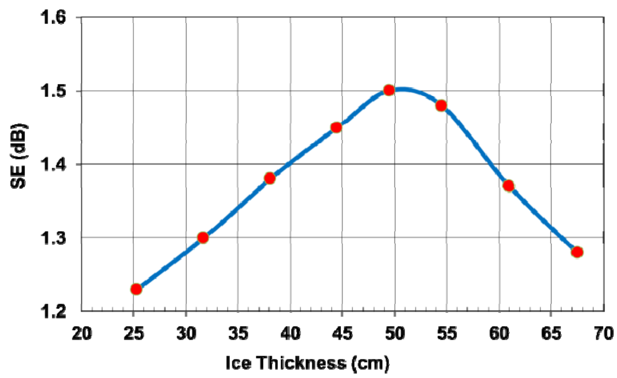

Figure 11. Plot of 8 minimum SE values (red circles) from Figure 10

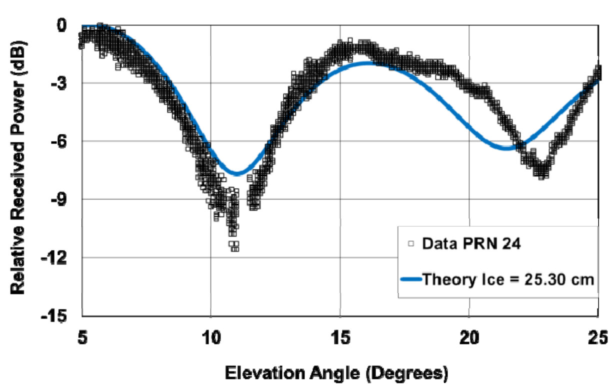

Figure 12. Elevation plots for PRN 24, measured (squares) and theoretical (line)

Table 3. Inferred values of lake ice thickness and SE using the GPS-IR method; *in situ* range value is also shown

Method	Ice Thickness (cm)	SE (dB)
GPS-IR PRN 10	38.0	0.63
GPS-IR PRN 2	22.4	0.93
GPS-IR PRN 24	25.3	1.23
in situ	39.4±1.3	

4. Conclusions

Lake ice thickness is an important parameter in the northern hemisphere. For example, the meteorogical conditions in the northern latitudes may be related to the ice thickness in lakes and rivers. Also, critical lake ice information (i.e., extent and duration) is important because it can have a major impact on the economy of this region. In particular, lake ice cover can impede commercial navigation; interfere with hydropower production and cooling water intakes; and damage shore structures. In addition, ice cover impacts the water balance of the lakes. This occurs because ice cover affects mass and energy transfers to the lakes and from the lakes. In short, better lake ice measurements will improve the understanding of ice cover climatology and forecasts of winter lake ecosystems.

A 1-day experiment was performed to investigate if it might be possible to estimate freshwater lake ice thickness by GPS-IR. A QNA produced an average inferred ice thickness of 38.0 cm from the track of GPS satellite PRN 10. This inferred ice thickness slightly underestimated the *in situ* measurements (39.4 cm ± 1.3 cm). Data from two other GPS satellite (PRNs 2 and 24) significantly underestimated the *in situ* measurements. It is strongly suspected that the lake ice thickness was uniform for some sections of the frozen reservoir while it was nonuniform for other sections of the reservoir. If this is the case, then the viability of this GPS-IR technique in inferring ice thickness is stongly dependent upon on a satellite's azimuth track across a frozen lake. In other words, one satellite azimuth track across a section of frozen lake may have uniform ice thickness, whereas another satellite track may not. Therefore, the validity of retrieving lake ice thickness with this simple model requires that the ice layer thickness be relativily uniform.

Future research will use this technique to estimate different lake ice thicknesses without snow cover and with snow cover. Also, several ice holes will be manually drilled within the antenna's first Fresnel zone in order to verify the actual ice thickness. These measurements will quantify the spatial variability of lake ice thickness which is critical for this GPS-IR technique. The height of the receiving antenna will be increased to ~ 2 m in order to reduce potential biases in estimating lake ice thickness (Larson & Nievinski, 2012; Gutmann, Larson, Williams, Nievinski, & Zavorotny, 2011; Larson et al., 2009). Future theoretical work will include two or more ice layers, variations of ice thickness in the antenna viewing area, and the antenna cross-polarization component.

In summary, if estimating freshwater lake ice thickness can be accomplished by GPS-IR then it may be more reasonable than using radar, radiometer or manually drilling. In addition, GPS-IR may provide better spatial and temporal coverage of lake ice thickness measurements than the current techniques.

Acknowledgments

The Montana State University Billings' (MSUB) Research and Creative Endeavor grant 630714, Dr. Tasneem Khaleel and Dr. Christine Shearer-Cremean of MSUB supported this work. Dr. M. McBride of MSUB, J. Jacobson (my Mother), W. Dotson (Keri Systems) and the Montana Department of Fish, Wildlife and Parks provided critical help with this research. The anonymous reviewers provided very valuable comments and suggestions which I am extremely grateful.

References

Apinis, J. J., & Peake, W. H. (1976). Passive microwave mapping of ice thickness. *Ohio State University Electro-Science Lab, Rep. 3892-2*, Columbus, OH.

Arcone, S. A. (1991). Dielectric constant and layer-thickness interpretation of helicopter-borne short-pulse radar waveforms reflected from wet and dry river-ice sheets. *IEEE Trans. Geosci. Remote Sensing, 29*(5), 768-777. http://dx.doi.org/10.1109/36.83992

Arcone, S. A., Yankielun, N. E., & Chacho, E. F., Jr. (1997). Reflection profiling of arctic lake ice using microwave FM-CW radar. *IEEE Trans. Geosci. Remote Sensing, 35*(2), 436-443.

http://dx.doi.org/10.1109/36.563282

Assel, R. A. (2004). Lake Erie ice cover climatology - basin averaged ice cover: winters 1898-2002. *NOAA Tech. Memo, GLERL-128*, Ann Arbor, MI.

Assel, R. A. (2005). Great Lakes weekly ice cover statistics. *NOAA Tech. Memo, GLERL-133*, Ann Arbor, MI.

Beckmann, P., & Spizzichino A. (1987). *The scattering of electromagnetic waves from rough surfaces.* Norwood, MA: Artech House.

Bengtsson, L. (1986). Spatial variability of lake ice covers. *Series A, Physical Geography, 68*(½) 113-121. http://dx.doi.org/10.2307/521182

Cardellach, E., Fabra, F., Nogues-Correig, O., Oliveras, S., Ribó, S., & Rius, A. (2011). GNSS-R ground-based and airborne campaigns for ocean, land, ice, and snow techniques: application to the GOLD-RTR data sets. *Radio Sci, 46*(4). http://dx.doi.org/10.1029/2011rs004683

Cooper, D. W., Mueller, R. A., & Schertler, R. J. (1976). Remote profiling of lake ice using an S-band short-pulse radar aboard an all-terrain vehicle. *Radio Sci., 11*(4), 375-381. http://dx.doi.org/10.1029/RS011i004p00375

Fabra, F., Cardellach, E., Nogu´es-Correig, Oliveras, S., Rib´o, S., Rius, A., … D'Addio, S. (2011). An empirical approach towards characterization of dry snowlayers using GNSS-R," *Proc. Int. Geosci. Remote Sens. Symp*, Vancouver, Canada, 4379 - 4382. http://dx.doi.org/10.1109/IGARSS.2011.6050202

Finlay, P. I., Parry, N. S., Proskin, S. A., & Mickle, R. J. (2008). An overview of ice profiling using ground penetrating radar (GPR). *21st Symp. Appl. Geophy. Engin. Environ. Probl. (SAGEEP)*, Philadelphia, PA., USA, 461-470.

Gleason, S., & Gebre-Egziabher, D. (2009). *GNSS applications and methods*. Artech House, Norwood.

Gleason, S., Lowe, S., & Zavorotny, V. (2009). *Remote sensing using bistatic GNSS reflections in GNSS applications and methods*. Artech House, Norwood.

Gutmann, E., Larson, K. M., Williams, M., Nievinski, F. G., & Zavorotny, V. (2011). Snow measurement by GPS interferometric reflectometry: An evaluation at Niwot Ridge, Colorado. *Hydrol Process 26*, 2951-2961. http://dx.doi.org/10.1002/hyp.8329

Hall, D. K., Fagre, D. B, Klasner, F., & Liston, G. E. (1994). Analysis of ERS 1 synthetic aperture radar data of frozen lakes in northern Montana and implications for climate studies. *Journal of Geophysical Research, 99*(Cll), 22, 473-22, 482. http://dx.doi.org/10.1029/94JC01391

Hall, D. K., Foster, J. L., Chang, A. T. C., & Rango, A. (1981). Freshwater ice thickness observations using passive microwave sensors. *IEEE Trans. Geosci. Remote Sensing, 19*(4), 189-193. http://dx.doi.org/10.1109/TGRS.1981.350371

Herceg, D., Krejic, N., & Luzanin, Z. (1996). Quasi-Newton's method with correction. *Novi Sad J. Math., 26*(1), 115-127.

Jacobson, M. D. (2008). Dielectric-covered ground reflectors in GPS multipath reception—theory and measurement. *IEEE Geosci. Remote Sens. Lett., 5*(3), 396–399. http://dx.doi.org/10.1109/lgrs.2008.917130

Jacobson, M. D. (2010). Snow-covered lake ice in GPS multipath reception—theory and measurement," *Advances in Space Research*, *46*(2), 221-227. http://dx.doi.org/10.1016/j.asr.2009.10.013

Jacobson, M. D. (2014). Estimating snow water equivalent estimation for a slightly tilted snow-covered prairie grass field by GPS interfermetric reflectometry. EURASIP Journal on Advances in Signal Processing. http://dx.doi.org/10.1186/1687-6180-2014-61

Jin, S., & Komjathy, A. (2010). GNSS reflectometry and remote sensing: new objectives and results. *Adv. Space Res., 46*(2), 111-117. http://dx.doi.org/10.1016/j.asr.2010.01.014

Jin, S., Feng, G. P., & Gleason, S. (2011). Remote sensing using GNSS signals: current status and future directions. *Adv. Space Res., 47*(10), 1645-1653. http://dx.doi.org/10.1016/j.asr.2011.01.036

Larson, K. M., & Nievinski, F. G. (2012). GPS snow sensing: results from the EarthScope plate boundary observatory. *GPS Solutions, 17*, 41-52. http://dx.doi.org/10.1007/s10291-012-0259-7

Larson, K. M., Gutmann, E., Zavorotny, V., Braun, J., Williams, M., & Nievinski, F. (2009). Can we measure snow depth with GPS receivers? *Geophys. Res. Lett., 36*. http://dx.doi.org/10.1029/2009gl039430

Mala Geoscience CX (2007). Quality inspections of ice roads using GPR. Printed matter no. 2899. Mala, Sweden. Retrieved from http://www.malags.com/getattachment/465a6999-c36c-46bc-80bc-2183c3b7ebb0/Case-Studies-1

Martinez, J. M. (1990). A family of quasi-Newton methods for nonlinear equations with direct secant updates of matrix factorizations. *SIAM J. Numer. Anal., 27*, 1034-1049. http://dx.doi.org/10.1137/0727061

Matzler, C., & Wegmuller, U. (1987). Dielectric properties of freshwater ice at microwave frequencies. *Journal of Physics D: Applied Physics, 20*, 1623-1630. http://dx.doi.org/10.1088/0022-3727/21/11/522

McCreight, J. L., Small, E. E., & Larson, K. M. (2014). Snow depth, density, and SWE estimates derived from GPS reflection data: validation in the Western U.S., *Water Resources Research*. http://dx.doi.org/10.1002/2014WR015561

Nievinski, F. G., & Larson, K. M. (2014a). Inverse modeling of GPS multipath for snow depth estimation, I: formulation and simulations, IEEE Trans. Geosci. Remote Sensing, *52*(10), 6555-6563. http://dx.doi.org/10.1109/TGRS.2013.2297681

Nievinski, F. G., & Larson, K. M. (2014b). Inverse modeling of GPS multipath for snow depth estimation, II: application and validation, *IEEE Trans. Geosci. Remote Sensing, 52*(10), 6564-6573. http://dx.doi.org/10.1109/TGRS.2013.2297688

Palecki, M. A., & Barry, R. G. (1986). Freeze-up and break-up of lakes as an index of temperature changes during the transition seasons: A case study in Finland. J. *Clim. Appl. Meteorol., 25*, 893-902. http://dx.doi.org/10.1175%2f1520-0450(1986)025%3c0893%3aFUABUO%3e2.0.CO%3b2

Riek, L., Crane, R. K., & O'Neill, K. (1990). A signal-processing algorithm for the extraction of thin freshwater-ice thickness from short pulse radar data. *IEEE Trans. Geosci. Remote Sensing, 28*(1), 137-145. http://dx.doi.org/10.1109/36.45751

Rodriguez-Alvarez, N., Aguasca, A., Valencia, E., Bosch-Lluis, X., Camps, A., Ramos-Perez, I., … Vall-llossera, M. (2012). Snow thickness monitoring using GNSS measurements. *IEEE Geosci. Remote Sens. Lett. 9*(6), 1109-1113. http://dx.doi.org/10.1109/lgrs.2012.2190379

Stutzman, W. L. (1993). *Polarization in electromagnetic systems.* Norwood, MA: Artech House.

Swift, C. T., Jones, W. L., J., Harrington, R. F., Fedors, J. C., & Couch, R. H. (1980). Microwave radar and radiometric remote sensing measurements of lake ice. *Geophys. Res. Letters, 7*(4), 243-246. http://dx.doi.org/10.1029%2fGL007i004p00243

Ulaby, F. T., Moore, R. K., & Fung, A. K. (1986). *Microwave remote sensing, active and passive, vol. I.* Norwood, MA: Artech House.